Department of Biopharmaceutics, School of Pharmacy, Hyogo University of Health Sciences, Kobe, Hyogo, Japan

Effect of miR-433-3p and miR-883b-5p on murine CYP 3A family enzymes in AML12 cells

Y. Sugino, F. Kugawa*

Received May 11, 2018, accepted June 15, 2018

**Corresponding author: Fumihiko Kugawa. Ph.D., Department of Biopharmaceutics, School of Pharmacy, Hyogo University of Health Sciences, 1-3-6 Minatojima, Chuo-Ku, Kobe, Hyogo 650-8530, Japan*
jfkugawa@huhs.ac.jp

Pharmazie 73: 519-525 (2018) *doi: 10.1691/ph.2018.8530*

Here we searched for microRNAs that could interact with cytochrome P450 (CYP) enzymes *in silico,* and then investigated their effects on *Cyp* gene expressions using the cultured mouse liver cell line AML12. Among the mouse *Cyp3a* genes, some miRNAs were found to interact with *Cyp3a11*, *13*, *16,* and *44* by the *in silico* analysis using the miRWalk2.0 database. In addition to this software, which included twelve miRNA target prediction algorithms, we also applied our in-house-developed Excel VBA algorithm to obtain predictions more efficiently. Finally, two miRNAs, miR-433-3p and miR-883b-5p, were extracted as candidates that interact with *Cyp3a* genes. To evaluate the effects of these miRNAs on *Cyp3a* gene expression, we first examined whether they actually interacted with the *Cyp3a 3'*-untranslated region (3'-UTR) using a luciferase assay system in AML12 cells. We then evaluated whether the expression of each miRNA affected the expression of *Cyp3a* mRNAs and their transcribed proteins. We found that the transiently expressed miRNAs significantly reduced the reporter activity of the *Cyp3a 3'*-UTR site in AML12 cells. In addition, the mRNA and protein expressions of the corresponding *Cyp3as* were significantly decreased in the miRNA-treated AML12 cells. Using cultured cells, we clearly demonstrated that miR-433-3p and miR-883b-5p, which were identified by *in silico* prediction, actually bind to *Cyp3a* mRNAs and regulate *Cyp* gene expressions.

1. Introduction

MicroRNAs (miRNAs) are small (about 20 nucleotides) non-coding RNAs that act as regulators of biological functions such as cell proliferation, differentiation, and development (Ambros 2004; Wienholds and Plasterk 2005). They bind to a miRNA recognition element (MRE) on the 3'-UTR of target mRNAs and elicit translational repression through target mRNA degradation (Barrett et al. 2012). As of late 2017, the number of deposited human miRNAs was over 2500, according to the miRBase depository data (http://www.mirbase.org/).

Each miRNA regulates multiple mRNAs, and each mRNA can be targeted by multiple miRNAs. Approximately 60% of the human mRNAs are estimated to be regulated by miRNAs (Friedman et al. 2009). Thus, it is likely that miRNAs are not only involved in various biological functions but also regulate the onset and progression of diseases. Consequently, if the relationship between a certain miRNA and its target mRNA can be predicted with high accuracy, it could have implications for the use of the such genes or proteins as therapeutic targets. Moreover, disease-associated miRNAs could be applied clinically as disease biomarkers in the near future. In this study, we focused on a group of genes that encode drug metabolic enzymes (cytochrome P450, or CYP), whose expression is known to be affected by some miRNAs.

A number of xenobiotics (including medicines) are metabolized by CYPs. Thus, it is important to understand the CYP-expression mechanisms not only because they are interesting from a molecular biological point of view, but also because they have implications for clinical therapies (Beaune 1993; Gonzalez 1988). The CYP expression is influenced by a variety of factors, including gender, age, hormones as internal factors, and xenobiotics as external factors, and also by the onset of disease. This means that conditions such as cancer onset or bacterial infection can cause fluctuations in CYP function *via* miRNA (Assenat et al. 2006; Chaluvadi et al. 2009). Recent clinical case reports showed that inflammation caused by bacterial infection can affect the function of hepatic CYP enzymes (Aitken and Morgan 2007; Yan et al. 2015); this finding generated a lot of attention. In addition, CYP-activity fluctuations have been reported from animal studies (Iber et al. 1999; Morgan 1997; Yang and Lee 2008). Given this background, in this study we sought to identify miRNAs that influence the CYP expression.

CYP is a well-known metabolic enzyme in the liver. Thus, researchers have long been interested in the relationship between CYP enzymes and drugs. Most of this research to date has focused on the "induction" or "inhibition" of CYP enzymes by drugs. However, we are interested in a different perspective instead of focusing on the "drugs" we are interested in the potential of "disease" to influence the CYP expression. In our previous reports, we revealed that the switching of inflammation-related signaling pathways was required for some CYP expressions (Moriya et al. 2012; Moriya et al. 2014). Such CYP regulations are likely to depend on direct interactions between miRNAs and *Cyp* mRNAs. However, it should be noted that nuclear receptors may also take part in CYP expression; in addition to the direct effect of miRNAs, the *Cyp* gene expression is known to be regulated by nuclear receptors such as PXR (Pregnane X Receptor) under xenobiotic treatment.

Thus, in the current study, we sought to identify miRNAs that control the expression of CYP molecular species by binding to the *Cyp* mRNAs directly or by affecting the expression of CYP nuclear receptors. The identification of miRNAs affecting the expression of CYP species may help elucidate the mechanisms behind the observed fluctuations in drug-metabolizing capability. In this study, we adopted a two-step research strategy. First, we identified miRNAs that were predicted to bind to the mouse *Cyp3a* 3'-noncoding region using the miRWalk2.0 software and our in-house-developed Excel VBA algorithm. Second, we performed experiments in cultured cells (AML12 cells) to investigate whether the *in silico*-predicted miRNAs could actually negatively regulate *Cap3a* genes.

2. Investigations and results

2.1. In silico extraction of miRNAs that could target each Cyp3a gene

To extract miRNA candidates, we used miRWalk2.0, a miRNA target-gene prediction database that is available online. This algorithm has the ability to predict miRNAs that bind the 3'-UTR region of a gene of interest, in our case that of individual *Cyp3a* genes. The number of miRNAs that were predicted to bind *Cyp3a* genes were 1226 for *Cyp3a11*, 1768 for *Cyp3a13*, 690 for *Cyp3a16,* and 1166 for *Cyp3a44* (Table 1).

Table 1: Number of miRNAs predicted to bind individual *Cyp3a* genes

Gene	Number of miRNAs
Cyp3a11	1226
Cyp3a13	1768
Cyp3a16	690
Cyp3a44	1166

Since these numbers of predicted miRNAs were enormous, we tried to narrow them down to obtain truly plausible candidates. MiRWalk2.0 includes 12 kinds of algorithms to detect the direct interaction between a miRNA and a *Cyp* mRNA. Therefore, we temporarily classified the candidate miRNAs as "tentative-positive" when 6 or more algorithms out of the 12 predicted positive binding between the miRNA and mRNA.

In addition, "duplication in binding," namely the binding of a certain miRNA to several *Cyp* mRNA members, could occur; or reversely, the binding of several miRNAs to one *Cyp* mRNA could also occur. To rule out these "false-positive" counts we developed an in-house-coded Excel VBA algorithm (data not shown). Using both *in silico* systems, we finally identified five miRNAs (miR-433-3p, miR-551b-5p, miR-691, miR-706, and miR-883b-5p) as tentative candidates for binding *Cyp3a* genes (Fig. 1).

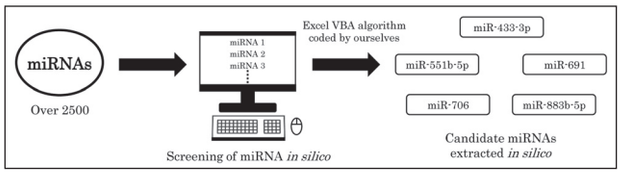

Fig. 1: Protocol for obtaining five candidate miRNAs

In the case of miR-433-3p, more than half of the algorithms (6 or 7) in miRWalk2.0 predicted its binding to four *Cyp3a* genes: *Cyp3a11*, *Cyp3a13*, *Cyp3a16,* and *Cyp3a44* (Table 2). For miR-883b-5p, eight algorithms predicted its binding to *Cyp3a11* and *Cyp3a44*, and 9 to *Cyp3a13*. However, only one algorithm predicted miR-883b-5p's binding to *Cyp3a16*, so we considered this binding to be negligible. Thus, miR-883b-5p had an unusually large number of algorithms that predicted its tentative binding to the target *Cyp3a* mRNA. Based on these analyses, we focused on two miRNAs, miR-433-3p and miR-883b-5p, as plausible candidates for further *in vitro* experiments examining the interaction between miRNA and *Cyp* mRNAs.Table 3 shows the predicted binding sites of miR-433-3p and miR-883b-5p in individual *Cyp3a* mRNAs obtained from the TargetScan algorithm (except for the binding site of miR-883b-5p to *Cyp3a16*, which was predicted by RNAhybrid). The predicted binding site of miR-433-3p (MRE433-3p) was located at positions 71 to 77 in the *Cyp3a11* 3'-UTR, from 2354 to 2360 in the *Cyp3a13* 3'-UTR, from 71 to 77 in the *Cyp3a16* 3'-UTR, and from 71 to 77 in the *Cyp3a44* 3'-UTR.

Table 2: Number of algorithms predicting miRNA *vs Cyp3a* gene binding

miRNA	Genes	Number of algorithms (out of 12)
mmu-miR-433-3p	*Cyp3a11*	6
	Cyp3a13	7
	Cyp3a16	7
	Cyp3a44	6
mmu-miR-551b-5p	*Cyp3a11*	1
	Cyp3a13	6
	Cyp3a16	6
	Cyp3a44	7
mmu-miR-691	*Cyp3a11*	6
	Cyp3a13	7
	Cyp3a16	1
	Cyp3a44	8
mmu-miR-706	*Cyp3a11*	6
	Cyp3a13	8
	Cyp3a16	0
	Cyp3a44	7
mmu-miR-883b-5p	*Cyp3a11*	8
	Cyp3a13	9
	Cyp3a16	1
	Cyp3a44	8

※Numbers in the rightmost column are the number of algorithms in miRWalk2.0 that predict the binding of the individual miRNA and the target *Cyp* gene.
※The miRNAs in the table are all from murine species.

Similarly, MRE-883b-5p's binding site was located at positions 155 to 161 in the *Cyp3a11* 3'-UTR, from 2152 to 2158 in the *Cyp3a13* 3'-UTR, from 155 to 161 in *Cyp3a44* 3'-UTR, and from position 93 to 99 from the transcription start site in *Cyp3a16*.

2.2. The two miRNAs bind to Cyp3a mRNAs to affect Cyp3a gene expressions

To examine whether miR-433-3p or miR-883b-5p actually binds to individual *Cyp3a* mRNAs, we constructed miRNA expression vectors (pBA/miRNA) and reporter vectors for the binding sites on mRNAs (pmirGLO/*Cyp3a* 3'-UTR), and performed luciferase assays. The constructed vectors were introduced into AML12 cells as described in the Experimental section, and then the *Cyp3a* mRNA expressions were evaluated as the luciferase activity.

Figure 2 shows the effect of miR-433-3p or miR-883b-5p on the gene expression of *Cyp3a11* (A), *Cyp3a13* (B), *Cyp3a16* (C), and *Cyp3a44* (D). Empty vector (pBA) or the individual miRNA-expression vectors, and the reporter vectors in which each *Cyp3a* 3'-UTR region was subcloned were transfected into AML12 cells, and then the luciferase activity was evaluated.

The empty pBA vector did not change any *Cyp3a* gene expressions (compare black bars and white bars in Fig. 2 (A) to (D)). When the pBA vector bearing miR-433-3p or miR-883b-5p was transfected into AML12 cells at different doses, the mRNA level of each *Cyp3a* gene was significantly decreased dose-dependently; with increasing miR-433-3p overexpression, the ratio of *Cyp3a11* to control decreased from 72.9 to 53.9% (Fig. 2A), that of *Cyp3a13* decreased from 83.6 to 53.3% (Fig. 2B), that of *Cyp3a16* decreased from 77.0 to 41.7% (Fig. 2C), and that of *Cyp3a44* decreased from 87.5 to 54.3% (Fig. 2D). Similarly, a dose-dependent decrease in luciferase activity was observed with miR-883b-5p overexpression; the *Cyp3a11* expression relative to control decreased from 71.7 to 42.6% (Fig. 2A), that of *Cyp3a13* decreased from 92.5 to 59.4% (Fig. 2B), that of *Cyp3a16* decreased from 75.9 to 59.2% (Fig. 2C), and that of *Cyp3a44* decreased from 93.8 to 64.1% (Fig. 2D).

These results clearly revealed that miR-433-3p and miR-883b-5p independently regulate the gene transcription of *Cyp3a* by recognizing and binding to the 3'-UTR of the four species of *Cyp3a* mRNA used this study.

Table 3: Predicted binding sites for miR-433-3p or miR-883b-5p in each target *Cyp3a* sequence

	miR-433-3p	miR-883b-5p
Cyp3a11 (2053bp)	Position 1664~1670 of *Cyp3a11* (Position 71~77 of *Cyp3a11* 3'-UTR) 5' -GACAUUUUAGUUUCAUCAUGAG- 3' UGUGGCUCCUCGGGUAGUACUA	Position 1748~1754 of *Cyp3a11* (Position 155~161 of *Cyp3a11* 3'-UTR) 5' -ACAUCCACUGAACUUUCUCAGUG- 3' ACUGACGAUGGGUAAGAGUCAU
Cyp3a13 (2955bp)	Position 2819~2825 of *Cyp3a13* (Position 2354~2360 of *Cyp3a13* 3'-UTR) 5' -AUUUACCTGCAAAAUUCAUGAU- 3' UGUGGCUCCUCGGGUAGUACUA	Position 2617~2623 of *Cyp3a13* (Position 2152~2158 of *Cyp3a13* 3'-UTR) 5' -CCUUCUUGCTAAACUUCUCAGUA- 3' ACUGACGAUGGGUAAGAGUCAU
Cyp3a16 (1730bp)	Position 1669~1675 of *Cyp3a16* (Position 71~77 of *Cyp3a16* 3'-UTR) 5' -GAACACUUUAGUCUCAUCAUGAA- 3' UGUGGCUCCUCGGGUAGUACUA	Position 93~99 of *Cyp3a16* 5' -CAGAGAUGAACCUAUUUUCAGCG- 3' ACUGACGAUGGGUAAGAGUCAU
Cyp3a44 (1962bp)	Position 1671~1677 of *Cyp3a44* (Position 71~77 of *Cyp3a44* 3'-UTR) 5' -AGACACUUUAGUUUCAUCAUGAG- 3' UGUGGCUCCUCGGGUAGUACUA	Position 1755~1761 of *Cyp3a44* (Position 155~161 of *Cyp3a44* 3'-UTR) 5' -ACAUCCACUGAGCUUUCUCAGUG- 3' ACUGACGAUGGGUAAGAGUCAU

2.3. Effect of miR-433-3p or miR-883b-5p overexpression on individual Cyp3a gene and CYP3A protein expressions

Figure 3 shows the effect of the two miRNA expressions on individual *Cyp3a* gene expressions. The expression of four *Cyp3a* mRNAs (*Cyp3a11*, *Cyp3a13*, *Cyp3a16,* and *Cyp3a44*) was evaluated by Real-Time PCR under the condition of miR-433-3p's or miR-883b-5p's over-expression.

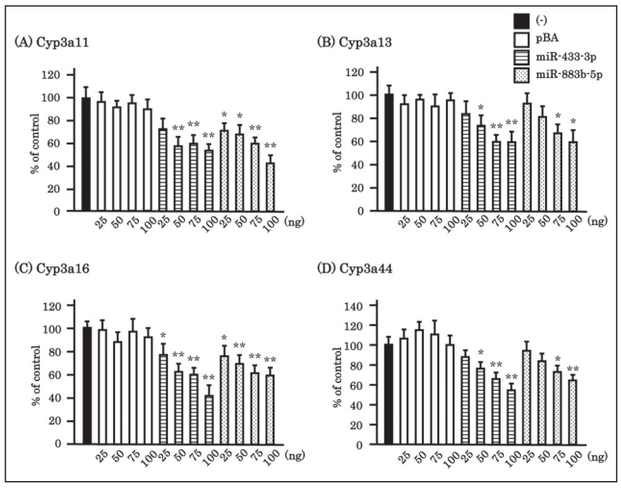

Fig. 2: Effect of miR-433-3p or miR-883b-5p on individual *Cyp3a* mRNA expressions AML12 cells were transiently co-transfected with a 20 ng equivalent volume of pmirGLO/*Cyp3a* 3'-UTR (reporter vector) and 0 to 100 ng equivalent volumes of pBA/miRNA vectors. Forty-eight hours after transfection, cells were harvested and a luciferase assay was conducted as described in the Experimental section. Luciferase activities from *Cyp3a11* 3'-UTR (A), *Cyp3a13* 3'-UTR (B), *Cyp3a16* 3'-UTR (C), and *Cyp3a44* 3'-UTR (D) relative to the activity in untreated cells (-), which was arbitrarily set as 100, are shown. Results show the mean±s.e. obtained from 6~8 independent experiments. $*P < 0.05$, $**P < 0.01$ vs. control (-)

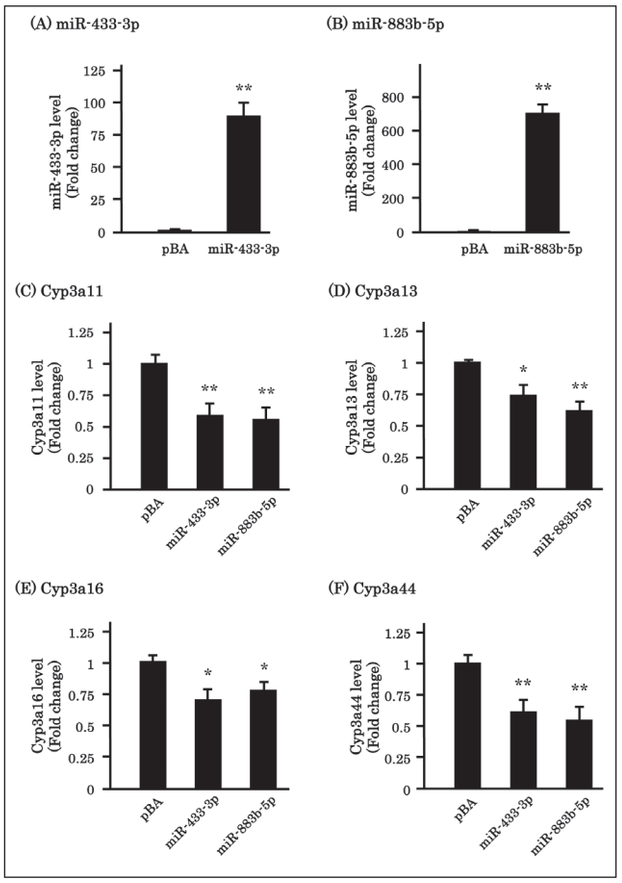

Fig. 3: Confirmation of the two miRNA expressions in AML12 cells and effect of miR-433-3p or miR-883b-5p over-expression on the mRNA expressions of individual *Cyp3a* genes. AML12 cells were transiently transfected with a 2-micro g equivalent volume of each pBA/miRNA vector. Forty-eight hours after transfection, the miR-433-3p (A) or miR-883b-5p (B) expression was assayed by Real-Time PCR. In panel (C) to (F), the individual mRNA levels of *Cyp3a11* (C), *Cyp3a13* (D), *Cyp3a16* (E), and *Cyp3a44* (F) were measured by Real-Time PCR. As a control, the empty pBA vector was transfected before Real-Time PCR. The expression level of each miRNA or the mRNA of each *Cyp3a* was normalized to that of U6 or Gapdh, respectively. The values relative to that of pBA alone, which was arbitrarily set as 1.0, are shown. Results show the mean±s.e. obtained from six independent experiments. $*P < 0.05$, $**P < 0.01$ vs. pBA

Figures 3 (A) and 3 (B) show that each miRNA expression vector markedly increased the miR-433-3p or miR-883b-5p expression level (89.9 times for miR-433-3p, 705.4 times for miR-883b-5p) compared to the pBA plasmid alone. Figures 3 (C) to 3 (F) show the reductions in *Cyp3a11* (C), *Cyp3a13* (D), *Cyp3a16* (E), and *CYP3A44* (F) mRNA under the overexpression of each of the two

miRNAs. In these figures, the expression level of individual *Cyp3a* genes in the presence of miRNA was normalized to the expression when the empty pBA vector was transfected. When miR-433-3p was introduced into the AML12 cells, the mRNA of each *Cyp3a* decreased, by 41.2% in the case of *Cyp3a11*, 26.2% for *Cyp3a13*, 30.2% for *Cyp3a16,* and 39% for *Cyp3a44*. Similar reductions in *Cyp3a* mRNA expression were observed under the over-expression of miR-883b-5p; the expression of *Cyp3a11* decreased by 44.6%, *Cyp3a13* by 38.5%, *Cyp3a16* by 22.5%, and *Cyp3a44* by 45.7%, compared to the control level.

Next, the protein expression of individual CYP3A enzymes was examined by Western blotting (Fig. 4). Since we could not obtain commercially available antibodies that specifically recognized the individual CYP3A enzymes used in this study, these experiments were conducted using an antibody that cross-reacts with CYP3A11 (Enzo Life Sciences, Inc.: BML-CR3310). Thus, we referred to "CYP3A protein" as a representative CYP3A enzyme in this Western blotting study.

The blots at the left in Fig. 4 show that the expression of CYP3A protein was clearly decreased when each of the two miRNAs was over-expressed. These results were quantified by densitometry scanning (Fig. 4, right), which showed that the CYP3A protein decreased to about 30% of the control level when miR-433-3p or miR-883b-5p was overexpressed.

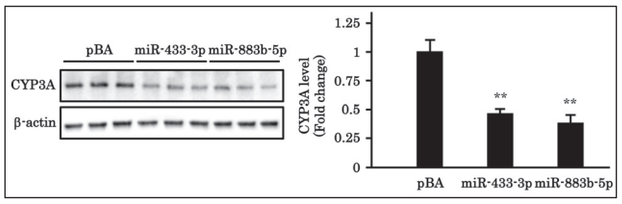

Fig. 4: Effect of miR-433-3p or miR-883b-5p over-expression on CYP3A protein expression. AML12 cells were transiently transfected with a 2-μg equivalent volume of each pBA/miRNA vector. Forty-eight hours after transfection, the total protein of the cells was extracted, and Western blotting was conducted to detect CYP3A enzymes. Panels at left show the Western blotting results indicating the CYP3A expression after the transduction of AML12 cells with each miRNA expression vector. Bar graph at right indicates the relative intensity of CYP3A signals shown at left, quantified with a densitometer. The expression levels of CYP3A protein relative to that of pBA alone, which was arbitrarily set as 1.0, are shown. Results show the mean±s.e. obtained from 6 independent experiments. Three lanes for each sample in the left panel show 3 representative results from 6 independent experiments. $^{**}P < 0.01$ VS. pBA

2.4. Effects of miR-433-3p or miR-883b-5p over-expression on Pregnane X Receptor (PXR) mRNA expression

The Pregnane X Receptor (PXR) is a nuclear receptor that is indispensable for *Cyp3a* gene expressions (Goodwin et al. 2002). Thus, we investigated the effects of miR-433-3p or miR-883b-5p over-expression on the mRNA and protein expression of PXR in AML12 cells (Figs. 5 and 6).

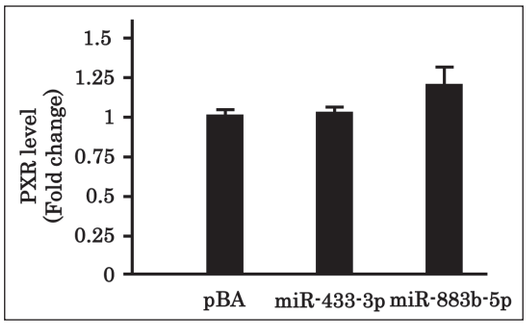

Fig. 5: Effect of miR-433-3p or miR-883b-5p over-expression on the mRNA expression of PXR. AML12 cells were transiently transfected with a 2-μg equivalent volume of each pBA/miRNA vector. Forty-eight hours after transfection, the mRNA expression level of PXR was measured by Real-Time PCR. The expression levels of PXR mRNA were normalized to that of Gapdh, and the values relative to that obtained with pBA alone, which was arbitrarily set as 1.0, are shown. Results show the mean±s.e. obtained from 6 independent experiments.

The PXR mRNA increased 101% compared to the control in the case of miR-433-3p overexpression and 122% in miR-883b-5p's case (Fig. 5). However, little change in the PXR protein expression was observed under the overexpression of either of the two miRNAs (Fig. 6). We presently have no reasonable explanation why

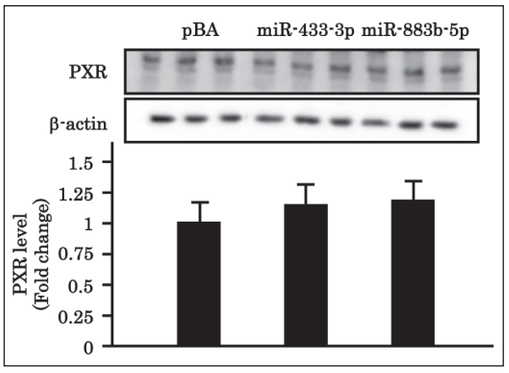

Fig. 6: Effect of miR-433-3p or miR-883b-5p over-expression on the protein expression of PXR. AML12 cells were transiently transfected with a 2-μg equivalent volume of each pBA/miRNA vector. Forty-eight hours after transfection, Western blotting was conducted to evaluate the expression of PXR protein. The relative intensity of the PXR protein band was quantified with a densitometer. The expression levels of PXR protein relative to that obtained with the pBA alone, which was arbitrarily set as 1.0, are shown. Results show the mean±s.e. obtained from 6 independent experiments. Three lanes for each sample in the top panel display three representative results from 6 independent experiments.

the PXR mRNA was somewhat increased after miR-883b-5p was over-expressed in AML12 cells. However, the results of PXR protein expressions indicated that the over-expression of miR-883b-5p had little or no effect on the *Cyp3a* gene expression *via* PXR.

Taking these results together, we concluded that the two tested miRNAs (miR-433-3p and miR-883b-5p) independently bound the 3'-UTR of individual *Cyp3a* mRNAs directly, resulting in decreased CYP3A enzyme expression in AML12 cultured cells.

3. Discussion

MiRNAs are non-coding RNAs that function to control gene expressions by suppressing post-transcriptional translation. They regulate many kinds of gene expressions besides the CYPs that were examined in this study. Several studies have reported that marked fluctuations in miRNA expressions *in vivo* are observed in cancer, heart diseases, and mental disorders such as depression; thus, it is likely that miRNAs regulate the progression of diseases or disorders (Gui et al. 2017; Pan and Liu 2015; Vegter et al. 2017). Among the various medical treatments available for a patient (surgery, radiation, psychotherapy, etc), drug treatment is usually the first considered and the most common. For example, for a runny nose we take an anti-allergy pill, for a headache we take a painkiller, etc. The important fact is that the enzyme most connected to drugs administered in the body is CYP. Thus, fluctuations in CYP enzyme expressions caused by medicines—namely, the induction or inhibition of CYP enzymes—has attracted the interest of researchers and physicians for years. On the other hand, a different perspective, how the disease itself affects the expression of drug-metabolizing enzymes (especially CYP enzymes), has been largely neglected by scientific and clinical researchers until recently.

To study the relationship between a disease and CYP enzymes, it is important to choose a surrogate marker that represents or is closely connected to the individual disease. For this purpose, we have been interested in miRNAs (Moriya et al. 2016). In the present study, we sought to identify miRNAs that have the potential to

change CYP enzyme activities. This research opens the possibility of predicting how various diseases/disorders influence a patients' CYP activities, and could be informative about the effectiveness of evidence-based drugs for an individual patient. However, these diseases/disorders are very diverse, and an enormous number of miRNAs is associated with them, which have been barriers to progress in this field.

For these reasons, we particularly focused on the interaction between miRNAs and CYP enzymes in this study. First, using an *in silico* method, we sought to extract miRNAs that would affect the expression of CYP enzymes. Then, using an *in vitro* cultured cell system, we sought to reveal the interactions between them.

Among the various CYP enzymes, we focused on four mouse CYP3A11 relatives, orthologs of human CYP3A4, that are strongly expressed in murine hepatic-derived AML12 cells: CYP3A11, CYP3A13, CYP3A16, and CYP3A44 (Fig. 7). Among the CYP enzymes, the CYP3A family is known to metabolize more than half of the species of xenobiotics, including drugs. Using our in-house-developed Excel VBA algorithm to narrow down the possible candidate miRNAs, we identified five miRNAs that had the potential to bind four *Cyp3a* genes. Finally, two of these miRNAs (miR-433-3p and miR-883b-5p) were investigated for their role in CYP3A enzyme expression.

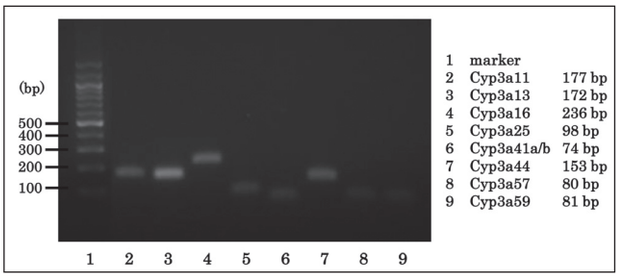

Fig. 7: Expression of mouse *Cyp3a* mRNAs in AML12 cells
The mRNA expressions of mouse *Cyp3a* genes in AML12 cells were examined by RT-PCR. Amplified products of *Cyp3a11* (177 bp; lane 2), *Cyp3a13* (172 bp; lane 3), *Cyp3a16* (236 bp; lane 4), *Cyp3a25* (98 bp; lane 5), *Cyp3a41a/b* (74 bp; lane 6), *Cyp3a44* (153 bp; lane 7), *Cyp3a57* (80 bp; lane 8), and *Cyp3a59* (81 bp; lane 9) after agarose gel electrophoresis are shown. Lane 1 indicates DNA markers. A representative result of 3 independent experiments is shown.

As shown in Fig. 2, both miR-433-3p and miR-883b-5p significantly decreased the luciferase activity in a reported assay by presumably binding to individual *Cyp3a* 3'-UTR regions. These results agreed well with the output from miRWalk's predictions. However, miR-883b-5p's predicted binding to *Cyp3a16* was relatively tentative, while it still decreased the reporter activity for this gene. Complementarity of the sequence between 2 to 7 bases from the 5' end (called the seed sequence) of a miRNA and that of its target mRNA 3'-UTR counterpart is thought to be critical for the miRNA-mRNA interaction (Barrett et al. 2012; Wienholds and Plasterk 2005). As shown in Table 3, the only predicted binding site of miR-883b-5p on the *Cyp3a16* gene by the miRWalk algorithm was on the 5'-UTR region of *Cyp3a16*. We cannot yet explain the reason for this result, but it is possible that the binding of miR-883b-5p to this 5'-UTR site directly or indirectly attenuates the mRNA expression of *Cyp3a16* by an as-yet unknown mechanism.

Alternatively, an interesting model was presented by Kawamata's group. They proposed that if a sequence from 12 to 16 bases on the 5' end of the miRNA is complementary to its target mRNA's sequence somewhere, the miRNA and its counterpart mRNA can stably bind to each other even if the seed sequence is not perfectly complementary (Kawamata et al. 2009; Yoda et al. 2010). Kawamata's model is worth considering for the binding discrepancy we observed in the present study.

Our Real-Time PCR and Western blotting experiments in Figs. 3 and 4 clearly indicated that both of the miRNAs interacted with the four tested *Cyp3a* mRNAs. The results of the reporter assays also clearly supported these findings. Although the miRNA expressions were evaluated after the transient transfection of miRNA expression vectors into AML12 cells in this study, we obtained similar results even after constructing AML12 cell lines that stably expressed the miRNAs. In experiments using these stable cell lines, the mRNA expression of each *Cyp3a* and the corresponding protein expressions of CYP3A were also significantly inhibited by the presence of each miRNA (data not shown). Collectively, our results clearly showed that the two miRNAs focused on in this study inhibited the expression of the four tested *Cyp3a* genes, at least in the cultured cell line AML12.

Some nuclear receptors are indispensable for the expression of *Cyp* genes. For the *Cyp3a* family gene expression, Pregnane X Receptor (or PXR) is required (Goodwin et al. 2002). In this case, a ligand (usually a xenobiotic) binds to PXR, which causes PXR to be activated and to form a heterodimer with Retinoic X Receptor (RXR). This heterodimer acts as a transcription factor for *Cyp3a* (Noble et al. 2006). Therefore, it was possible that the two miRNAs identified in this study influenced the PXR receptor expression by binding to the PXR mRNA. To investigate this possibility, we conducted the experiments shown in Figs. 5 and 6.

The Real-Time PCR in Fig. 5 clearly showed that neither miR-433-3p nor miR-883b-5p affected the mRNA expression of PXR (Fig. 5). In addition, the Western blotting data in Fig. 6 showed that the amount of PXR protein was not changed by the over-expression of either miRNA. These results strongly supported our proposal that the two miRNAs of interest suppress the expression of *Cyp3a*s, not *via* the PXR receptor but by directly binding to *Cyp3a* mRNAs, resulting in CYP3A enzyme inhibition.

miR-433-3p and its cousin miR-433 are reported to be involved in various biological functions, including cell differentiation, development, and cell survival (Gotanda et al. 2013; Luo et al. 2009; Sun et al. 2017; Tan et al. 2014). Among these reports, Tan's study showing that miR-433-3p is upregulated in the blood of hepatic cirrhosis patients is particularly interesting. miR-433 is reported to be expressed in the brain, stomach, and liver (Guo et al. 2013; Hua et al. 2012; Wang et al. 2012). The fact that the liver is among miR-433's expression sites has important implications, because the miR-433 family miRNAs, especially the miR-433-3p identified in this study, might be a useful surrogate biomarker for the healthy hepatic condition. Moreover, since our present results showed that miR-433-3p regulates *Cyp3a* gene expressions, at least in a cultured cell line, miR-433-3p might be a prominent biomarker for predicting the prognosis of a patient undergoing medical treatment for a liver disease such as liver cancer.

Regarding miR-883b-5p, there are almost no reports on its biological functions to date. The only exception is Sun's report showing that miR-883b-5p is involved in the protective effects of sevoflurane against neuronal damage under hypoxia *in vitro* (Sun et al. 2015). Therefore, little is known about target genes of miR-883b-5p or about diseases/disorders that are closely related to this miRNA. Thus, the results obtained in this study (namely, its regulation of *Cyp3a* expressions) reveal a novel function of miR-883b-5p.

In this study, we revealed that two computationally extracted miRNAs (miR-433-3p and miR-883b-5p) bind to *Cyp3a* genes and regulate their expression in a cultured cell system. Since CYPs are important enzymes in drug metabolism, understanding the detailed regulation of *Cyp* genes by certain miRNAs may improve our ability to predict the prognosis of diseases/disorders related to fluctuations in drug-metabolizing enzymes. In other words, this study provides basic research for the proper administration of therapeutic drugs for individuals suffering from certain diseases or from multiple disorders, such as elderly patients.

4. Experimental

4.1. Chemicals and reagents

All of the chemicals and regents for the cell-culture experiments, common biochemical experiments (for example, SDS-PAGE and Western-blotting), molecular biological experiments (for example, reverse transcription and Real-time PCR) were purchased from domestic or international laboratory reagent suppliers, and their grade was superfine.

The FuGENE HD, pmirGLO vector, and Dual-Glo Luciferase Assay system were purchased from Promega (Madison, WI, USA). The pBA-si hU6 vector, Dra I, Xho I, BamHI, and Hind III were purchased from TaKaRa Bio (Shiga, Japan). The

anti-CYP3A antibody was purchased from Enzo Life Science, Inc. (NY, USA). The anti-Pregnane X Receptor (PXR) antibody was purchased from Proteintech (Rosemont, IL, USA). The anti-β-actin antibody was purchased from Imgenex (San Diego, CA, USA). The horseradish peroxidase (HRP)-conjugated anti-rabbit IgG polyclonal antibody was purchased from R&D Systems, Inc. (Minneapolis, MN, USA). All primers were purchased from Fasmac (Kanagawa, Japan) and Invitrogen (Grand Island, NY, USA). The primer sequences are shown in Supplemental tables 1 to 3.

4.2. Cell culture

The murine hepatocyte AML12 cell line was maintained in Dulbecco's modified Eagle's medium and Ham's F12 medium (Wako) supplemented with 10% heat-inactivated fetal bovine serum (Equitech-Bio, Inc. TX, USA), 0.05 mg/mL insulin, 0.05 mg/mL transferrin, 0.05 ng/mL selenite, and 40 ng/mL dexamethasone, with 5% CO_2 at 37 °C. The cells were used at 1×10^5/well in 96-well tissue culture plates for the luciferase assay, and at 4.5×10^5/dish in 60-mm-diameter dishes for extracting total RNAs for Reverse-Transcription Polymerase Chain Reaction (RT-PCR) and Real-time PCR experiments, and for obtaining proteins for Western blotting experiments.

4.3. Production of cDNA from total RNAs

Total RNA was isolated from AML12 cells using ISOGEN II (Nippon Gene, Tokyo, Japan). Reverse-transcription to produce the cDNA for each miRNA was conducted using the miScript II RT Kit (Qiagen, Venlo, the Netherlands). Briefly, 0.5 μg of total RNA from AML12 cells was suspended in 20 μL of reaction buffer with miScript Reverse-Transcriptase and then incubated for 60 min at 37 °C. Reverse-transcription was stopped by heating the reaction mixture at 95 °C for 5 min.

Table 4: Primers designed for RT-PCR

Primer		Sequence
Cyp3a11	forward	5'-CAG CTT GGT GCT CCT CTA CC-3'
Cyp3a11	reverse	5'-TCA AAC AAC CCC CAT GTT TT-3'
Cyp3a13	forward	5'-GAC GAT TCT TGC TTA CCA GAA GG-3'
Cyp3a13	reverse	5'-CCG GTT TGT GAA GGT AGA GTA AC-3'
Cyp3a16	forward	5'-TGT CCT TGT CAG TAG CAC TCT-3'
Cyp3a16	reverse	5'-TGT GAT CTC GAT TTC AGA AAG GG-3'
Cyp3a25	forward	5'-CAA GCA CTT CCA TTT CCC TC-3'
Cyp3a25	reverse	5'-CTT ATT GGG CAG AGT TCT GTC-3'
Cyp3a41a/b	forward	5'-GCC AAA GGG ATT TTA AGA GTT GAC T-3'
Cyp3a41a/b	reverse	5'-GGT GTC AGG AAT GGA AAA AGT ACA-3'
Cyp3a44	forward	5'-ATC CCC AAA GGG TCA ATG GTG-3'
Cyp3a44	reverse	5'-TCC AAT TCC AAA GGG CAG ATA TAC G-3'
Cyp3a57	forward	5'-TGG AGG CCT GAA CTG CTA AAG-3'
Cyp3a57	reverse	5'-TAA CCA GCA GCA CCC AGG TT-3'
Cyp3a59	forward	5'-AGA GAC TTA GAA CAC TCC TG-3'
Cyp3a59	reverse	5'-CTC CAT ACT GTC TCA TGA TG-3'

The cDNA for each *Cyp3a* gene was synthesized from the total RNA of AML12 cells using the PrimeScript RT reagent Kit (TaKaRa Bio). Briefly, 0.5 μg of total RNA was suspended in 20 μL of reaction buffer with PrimeScript RT enzyme and then incubated for 15 min at 37 °C. Reverse transcription was stopped by denaturing the enzyme at 85°C for 5 s.

4.4. RT-PCR for examining the Cyp3a gene expressions in AML12 cells

Using the reverse-transcribed product of the total RNA from AML12 cells as a template, PCR was performed under the following conditions: 10 μM *Cyp3a*-specific forward and reverse primers (Supplement table 1) and the templates were mixed with TaKaRa Ex Taq. After thermal denaturation at 94 °C for 30 s, the chain reaction was performed for 30 cycles of 10 s at 98 °C, 30 s at 55 °C, and 30 s at 70 °C, followed by an extension reaction at 72 °C for 7 min. The PCR product was subjected to electrophoresis on a 2% agarose gel and visualized under UV light (260 nm).

4.5. Constructions of reporter vectors for luciferase reporter assays and of miRNA expression vectors

4.5.1 In silico prediction of miRNAs with the potential to bind Cyp3a genes

All of the *Cyp3a* genes examined were of mouse origin. The AML12 cells are derived from mouse liver. To predict which miRNAs had the potential to bind each *Cyp3a* gene of interest, we used the miRWalk2.0 software (instructions at http://zmf.umm.uni-heidelberg.de/apps/zmf/mirwalk2/). The prediction method used the following the criteria: minimum seed length of miRNA was seven, and a p-value<0.05 was considered significant. Twelve miRNA target prediction algorithms [miRWalk (Dweep et al. 2011), Microt4 (Paraskevopoulou et al. 2013), miRanda (Betel et al. 2010), miRBridge (Tsang et al. 2010), miRDB (Wang and EI Naqa 2008), miRMap (Vejnar et al. 2013), miRNAMap (Hsu et al. 2008), PicTar2 (Anders et al. 2012), PITA (Kertesz et al. 2007), RNA22 (Loher and Rigoutsos 2012), RNAhybrid (Rehmsmeier et al. 2004), and TargetScan (Friedman et al. 2009)] in the miRWalk software were used for the miRNA *vs. Cyp* mRNA binding prediction.

Table 5: Primers designed for expression vectors

Primer		Sequence
mmu-miR-433-3p	forward	5'-GAT CCG ATC ATG ATG GGC TCC TCG GTG TGT GTG CTG TCC ACA CCG AGG AGC CCA TCA TGA TCT TTT TTA-3'
mmu-miR-433-3p	reverse	5'-AGC TTA AAA AAG ATC ATG ATG GGC TCC TCG GTG TGG ACA GCA CAC ACA CCG AGG AGC CCA TCA TGA TCG-3'
mmu-miR-883b-5p	forward	5'-GAT CCG TAC TGA GAA TGG GTA GCA GTC AGT GTG CTG TCC TGA CTG CTA CCC ATT CTC AGT ACT TTT TTA-3'
mmu-miR-883b-5p	reverse	5'-AGC TTA AAA AAG TAC TGA GAA TGG GTA GCA GTC AGG ACA GCA CAC TGA CTG CTA CCC ATT CTC AGT ACG-3'
Cyp3a11 3'-UTR	forward	5'-TCA AGG AGT TCT TCT GAG TTC-3'
Cyp3a11 3'-UTR	reverse	5'-CTA GAG TTG TTA CAA GAG CTC A-3'
Cyp3a13 3'-UTR	forward	5'-CTA AGT GGA TTC AAG CAT CCT-3'
Cyp3a13 3'-UTR	reverse	5'-TCA CCC AAA GAA TGG ATA CAG-3'
Cyp3a16 3'-UTR	forward	5'-CTT GAG GAG TTC TGC TGA GTT-3'
Cyp3a16 3'-UTR	reverse	5'-GCA TCA AAA TCA ATC AGT TAA GC-3'
Cyp3a44 3'-UTR	forward	5'-TCA AGG AGT TCT TCT GAG TTC-3'
Cyp3a44 3'-UTR	reverse	5'-TGG ATA GAG ATG ATC CCA TG-3'

4.5.2 Construction of vectors

To construct the reporter vectors, Each *Cyp3a* 3'-UTR region was amplified by PCR using the reverse-transcribed products from the total RNA of AML12 cells as templates. The primers used in this experiment, "*Cyp3a* 3'-UTR forward primer" and "reverse primer" are shown in Supplement table 2. After thermal denaturation at 94 °C for 30 s, the chain reaction was performed with 30 cycles of 10 s at 98 °C, 30 s at 55 °C, and 30 s at 70 °C, followed by an extension reaction at 72 °C for 7 min. The amplified fragments of the *Cyp3a* 3'-UTR regions and the pmirGLO vector were both digested by Dra I and Xho I. The inserts were then subcloned into the pmirGLO vector to obtain pmirGLO/*Cyp3a* 3'-UTR vectors.

To construct the miRNA expression vectors, each miRNA oligonucleotide was produced by PCR using forward and reverse primers for each miRNA (Supplement table 2). The amplified oligonucleotides were then subcloned into the pBAsi-hU6 vector, at BamHI and Hind III sites, resulting in pBA/miRNA vectors.

Table 6: Primers designed for real-time PCR

Primer		Sequence
U6		5'-ACG CAA ATT CGT GAA GCG TT-3'
mmu-miR433-3p		5'-ATC ATG ATG GGC TCC TCG GTG T-3'
mmu-miR883b-5p		5'-TAC TGA GAA TGG GTA GCA GTC A-3'
Gapdh	forward	5'-AAC TTT GGC ATT GTG GAA GG-3'
Gapdh	reverse	5'-GGA TGC AGG GAT GAT GTT CT-3'
Cyp3a11	forward	5'-CAG CTT GGT GCT CCT CTA CC-3'
Cyp3a11	reverse	5'-TCA AAC AAC CCC CAT GTT TT-3'
Cyp3a13	forward	5'-GAC GAT TCT TGC TTA CCA GAA GG-3'
Cyp3a13	reverse	5'-CCG GTT TGT GAA GGT AGA GTA AC-3'
Cyp3a16	forward	5'-TGT CCT TGT CAG TAG CAC TCT-3'
Cyp3a16	reverse	5'-TGT GAT CTC GAT TTC AGA AAG GG-3'
Cyp3a44	forward	5'-ATC CCC AAA GGG TCA ATG GTG-3'
Cyp3a44	reverse	5'-TCC AAT TCC AAA GGG CAG ATA TAC G-3'
PXR	forward	5'-GAT GGA GGT CTT CAA ATC TGC-3'
PXR	reverse	5'-CAG CCG GAC ATT GCG TTT C-3'

4.6. Luciferase assay

A 20-ng equivalent volume of luciferase reporter vector and 0- to 100-ng equivalent volumes of each miRNA expression vector were co-transfected into AML12 cells using FuGENE HD, according to supplier's recommended protocol. After a 48-h incubation, the cells were harvested and lysed with PLB buffer by a conventional method. The luciferase activity was then measured by SpectraMax L (Molecular Devices, Tokyo, Japan) using the Dual-Glo Luciferase assay system.

4.7. Real-Time PCR

The expressions of the two miRNAs (miR-433-3p and miR-883b-5p) and of the mRNAs of individual *Cyp3a* genes (*Cyp3a11*, *Cyp3a13*, *Cyp3a16,* and *Cyp3a44*) were all measured by Real-Time PCR using the ABI 7500 Fast system (Applied Biosystems, CA, USA).

Real-Time PCR for each miRNA expression was carried out using 10 mM miRNA-specific forward primer (Supplement table 3) and 10×miScript Universal Primer in the miScript SYBR Green PCR Kit (Qiagen) as the reverse primer. The reaction was performed according to the manufacturer's protocol; the initial denaturation was 15 min at 95 °C, followed by 40 cycles of 15 s at 94 °C, 30 s at 55 °C, and 34 s at 70 °C chain reactions. The expressed miRNA levels were calculated from a relative standard curve and normalized to that of *U6* in the same sample.

The mRNA expression of each *Cyp3a* gene was also determined by Real-Time PCR with 10 μM *Cyp3a*-specific forward and reverse primers (Supplement table 3) in the SYBR Premix Ex Taq II (TaKaRa Bio) system. The reaction was performed according to the manufacturer's protocol; the initial denaturation was 30 s at 95 °C, followed by 40 cycles of 5 s at 95 °C and 34 s at 60 °C chain reactions. The mRNA levels of *Cyp3a* were calculated from a relative standard curve and normalized to that of glyceraldehyde-3-phospate dehydrogenase (Gapdh) in the same sample.

4.8. Western blotting

The extracted total protein from AML12 cell lysate (equivalent to 15 μg protein) was separated by SDS-PAGE (200 V, 30 min) and then blotted onto a PVDF membrane at 0.35 A for 1 h. The membrane was blocked with 1% non-fat dry milk/Tris-buffered saline (TBS)-0.05% Tween-20 (TBS-T) for 1 h, and then incubated with an anti-CYP3A polyclonal antibody (1:2000 dilution) or anti-PXR polyclonal antibody (1:1000 dilution) overnight at 4 °C. The membrane was rinsed 3 times with TBS-T buffer and then incubated with HRP-conjugated anti-rabbit IgG polyclonal antibody (1:2000 dilution) for 2 h at room temperature. Signals were detected with the Clarity Western ECL Substrate (Bio-Rad, Hercules, CA, USA), and blots were analyzed with an Image Quant Imager 400/400Lumi (GE Healthcare Japan, Tokyo, Japan). The CYP3A and PXR protein levels were normalized to b-actin in the same sample.

4.9. Statistical analysis

All experimental results were obtained from 6 to 8 independent experiments and are presented as the mean±S.E. The results from the various experimental groups and their corresponding controls were compared using Student's t-test. Differences were considered significant when $P < 0.05$.

Conflicts of interest: None declared.

References

Aitken AE, Morgan ET (2007) Gene-specific effects of inflammatory cytokines on cytochrome P450 2C, 2B6 and 3A4 mRNA levels in human hepatocytes. Drug Metab Dispos 35: 1687-1693.

Ambros V (2004) The functions of animal microRNAs. Nature 431: 350-355.

Anders G, Mackowiak SD, Jens M, Maaskola J, Kuntzagk A, Rajewsky N, Landthaler M, Dieterich C (2012) doRiNA: a database of RNA interactions in post-transcriptional regulation. Nucleic Acids Res 40: D180-186.

Assenat E, Gerbal-chaloin S, Maurel P, Vilarem MJ, Pascussi JM (2006) Is nuclear factor kappa-B the missing link between inflammation, cancer and alteration in hepatic drug metabolism in patients with cancer? Eur J Cancer 42: 785-792.

Barrett LW, Fletcher S, Wilton SD (2012) Regulation of eukaryotic gene expression by the untranslated gene regions and other non-coding elements. Cell Mol Life Sci 69: 3613-3634.

Beaune P (1993) [Human cytochromes P450. Applications in pharmacology]. Therapie 48: 521-526.

Betel D, Koppal A, Agius P, Sander C, Leslie C (2010) Comprehensive modeling of microRNA targets predicts functional non-conserved and non-canonical sites. Genome Biol 11: R90.

Chaluvadi MR, Kinloch RD, Nyagode BA, Richardson TA, Raynor MJ, Sherman M, Antonovic L, Strobel HW, Dillehay DL, Morgan ET (2009) Regulation of hepatic cytochrome P450 expression in mice with intestinal or systemic infections of citrobacter rodentium. Drug Metab Dispos 37: 366-374.

Dweep H, Sticht C, Pandey P, Gretz, N (2011) miRWalk--database: prediction of possible miRNA binding sites by "walking" the genes of three genomes. J Biomed Inform 44: 839-847.

Friedman RC, Farh KK, Burge CB, Bartel DP (2009) Most mammalian mRNAs are conserved targets of microRNAs. Genome Res 19: 92-105.

Gonzalez FJ (1988) The molecular biology of cytochrome P450s. Pharmacol Rev 40: 243-288.

Goodwin B, Redinbo MR, Kliewer SA (2002) Regulation of cyp3a gene transcription by the pregnane x receptor. Annu Rev Pharmacol Toxicol 42:1-23.

Gotanda K, Hirota T, Matsumoto N, Ieiri I (2013) MicroRNA-433 negatively regulates the expression of thymidylate synthase (TYMS) responsible for 5-fluorouracil sensitivity in HeLa cells. BMC Cancer 13: 369.

Gui B, Hsieh CL, Kantoff PW, Kibel AS, Jia L (2017) Androgen receptor-mediated downregulation of microRNA-221 and -222 in castration-resistant prostate cancer. PLoS One 12: e0184166.

Guo LH, Li H, Wang F, Yu J, He JS (2013) The Tumor Suppressor Roles of miR-433 and miR-127 in Gastric Cancer. Int J Mol Sci 14: 14171-14184.

Hsu SD, Chu CH, Tsou AP, Chen SJ, Chen HC, Hsu PW, Wong YH, Chen YH, Chen GH, Huang HD (2008) miRNAMap 2.0: genomic maps of microRNAs in metazoan genomes. Nucleic Acids Res 36: D165-169.

Hua D, Mo F, Ding D, Li L, Han X, Zhao N, Foltz G, Lin B, Lan Q, Huang Q (2012) A catalogue of glioblastoma and brain MicroRNAs identified by deep sequencing. OMICS 16: 690-699.

Iber H, Sewer MB, Barclay TB, Mitchell SR, Li T, Morgan ET (1999) Modulation of drug metabolism in infectious and inflammatory diseases. Drug Metab Rev 31: 29-41.

Kawamata T, Seitz H, Tomari Y (2009) Structural determinants of miRNAs for RISC loading and slicer-independent unwinding. Nat Struct Mol Biol 16: 953-960.

Kertesz M, Iovino N, Unnerstall U, Gaul U, Segal E (2007) The role of site accessibility in microRNA target recognition. Nat Genet 39: 1278-1284.

Loher P, Rigoutsos I (2012) Interactive exploration of RNA22 microRNA target predictions. Bioinformatics 28: 3322-3323.

Luo H, Zhang H, Zhang Z, Zhang X, Ning B, Guo J, Nie N, Liu B, Wu X. (2009) Down-regulated miR-9 and miR-433 in human gastric carcinoma. J Exp Clin Cancer Res 28: 82.

Morgan ET (1997) Regulation of cytochromes P450 during inflammation and infection. Drug Metab Rev 29: 1129-1188.

Moriya N, Kataoka H, Fujino H, Nishikawa J, Kugawa F (2012) Effect of lipopolysaccharide on the xenobiotic-induced expression and activity of hepatic cytochrome P450 in mice. Biol Pharm Bull 35: 473-480.

Moriya N, Kataoka H, Fujino H, Nishikawa J, Kugawa F (2014) Different expression patterns of hepatic cytochrome P450 s during anaphylactic or lipopolysaccharide-induced inflammation. Pharmazie 69: 142-147.

Moriya N, Kataoka H, Nishikawa J, Kugawa F (2016) Identification of candidate target Cyp genes for microRNAs whose expression is altered by PCN and TCPOBOP, representative ligands of PXR and CAR. Biol Pharm Bull 39: 1381-1386.

Noble SM, Carnahan VE, Moore LB, Luntz T, Wang H, Ittoop OR, Stimmel JB, Davis-Searles PR, Watkins RE, Wisely GB, LeCluyse E, Tripathy A, McDonnell DP, Redinbo MR (2006) Human PXR forms a tryptophan zipper-mediated homodimer. Biochemistry 45: 8579–8589.

Pan B, Liu Y (2015) Effects of duloxetine on microRNA expression profile in frontal lobe and hippocampus in a mouse model of depression. Int J Clin Exp Pathol 8: 15454-15461.

Paraskevopoulou MD, Georgakilas G, Kostoulas N, Vlachos IS, Vergoulis T, Reczko M, Filippidis C, Dalamagas T, Hatzigeorgiou AG (2013) DIANA-microT web server v5.0: service integration into miRNA functional analysis workflows. Nucleic Acids Res 41: W169-173.

Rehmsmeier M, Steffen P, Hochsmann M, Giegerich R (2004) Fast and effective prediction of microRNA/target duplexes. RNA 10: 1507-1517.

Sun S, Wang X, Xu X, Di H, Du J, Xu B, Wang Q, Wang J (2017) MiR-433-3p suppresses cell growth and enhances chemosensitivity by targeting CREB in human glioma. Oncotarget 8: 5057-5068.

Sun Y, Li Y, Liu L, Wang Y, Xia Y, Zhang L, Ji X (2015) Identification of miRNAs involved in the protective effect of sevoflurane preconditioning against hypoxic injury in PC12 Cells. Cell Mol Neurobiol 35: 1117-1125.

Tan Y, Ge G, Pan T, Wen D, Chen L, Yu X, Zhou X, Gan J (2014) A serum microRNA panel as potential biomarkers for hepatocellular carcinoma related with hepatitis B virus. PLoS One 9: e107986.

Tsang JS, Ebert MS, van Oudenaarden A (2010) Genome-wide dissection of microRNA functions and cotargeting networks using gene set signatures. Mol Cell 38: 140-153.

Vegter EL, Ovchinnikova ES, Silljé HHW, Meems LMG, van der Pol A, van der Velde AR, Berezikov E, Voors AA, de Boer RA, van der Meer P (2017) Rodent heart failure models do not reflect the human circulating microRNA signature in heart failure. PLoS One 12: e0177242.

Vejnar CE, Blum M, Zdobnov EM (2013) miRmap web: Comprehensive microRNA target prediction online. Nucleic Acids Res 41: W165-168.

Wang W, Zhao LJ, Tan YX, Ren H, Qi ZT (2012) Identification of deregulated miRNAs and their targets in hepatitis B virus-associated hepatocellular carcinoma. World J Gastroenterol 18: 5442-5453.

Wang X, El Naqa IM (2008) Prediction of both conserved and nonconserved microRNA targets in animals. Bioinformatics 24: 325-332.

Wienholds E, Plasterk RH (2005) MicroRNA function in animal development. FEBS Lett 579: 5911-5922.

Yan T, Lu L, Xie C, Chen J, Peng X, Zhu L, Wang Y, Li Q, Shi J, Zhou F, Hu M, Liu Z (2015) Severely impaired and dysregulated cytochrome P450 expression and activities in hepatocellular carcinoma: implications for personalized treatment in patients. Mol Cancer Ther 14: 2874-2886.

Yang KH, Lee MG (2008) Effects of endotoxin derived from Escherichia coli lipopolysaccharide on the pharmacokinetics of drugs. Arch Pharm Res 31: 1073-1086.

Yoda M, Kawamata T, Paroo Z, Ye X, Iwasaki S, Liu Q, Tomari Y (2010) ATP-dependent human RISC assembly pathways. Nat Struct Mol Biol 17: 17-23.